JOURNAL OF SPACECRAFT AND ROCKETS
Vol. 29, No. 3, May-June 1992

Hybrid Navier-Stokes/Monte Carlo Method for Reacting Flow Calculations

Frederik J. de Jong,* Jayant S. Sabnis,† Richard C. Buggeln,* and Henry McDonald‡
Scientific Research Associates, Inc., Glastonbury, Connecticut 06033

The axisymmetric hypersonic flow about a blunt-faced cylindrical forebody has been simulated using a newly developed hybrid Navier-Stokes/Monte Carlo method. This method couples a statistical ("Monte Carlo") treatment of the chemical reactions with a continuum ("Navier-Stokes") description of the gas mixture and the species transport. It facilitates the inclusion of more accurate chemical reaction models, surface catalytic reactions, etc., based on the use of collision/reaction cross sections (or probabilities), while it retains most of the run-time advantages of a full continuum method. The computed results have been compared with results obtained using a full continuum method and those of a direct simulation Monte Carlo method.

Nomenclature

c_p	= specific heat at constant pressure
D	= diffusivity
h	= enthalpy
h_f	= enthalpy of formation
h_0	= stagnation enthalpy
j	= diffusional mass flux
k	= thermal conductivity
$k_{AB}(T), k_{CD}(T)$	= rate coefficients
ℓ	= mixing length
M	= molecular weight
N	= number of species in the mixture
n	= number density
p	= pressure
R	= universal gas constant
T	= temperature
t	= time
U	= velocity
X	= mole fraction
Y	= mass fraction
μ	= viscosity
ρ	= density
τ	= stress tensor (molecular and turbulent)

Subscripts

A,B,C,D	= corresponding to species A, B, C, and D, respectively
i,j	= corresponding to species i and j, respectively

I. Introduction

SIMULATION of the aerothermal environment, including chemical reactions, around hypersonic vehicles at high altitudes has numerous applications. The temperature distribution around a hypersonic vehicle is of direct significance to the design of the thermal protection system. Furthermore, the high temperatures that will occur behind the bow shock will lead to dissociation, and possibly even ionization, of the air. Hence, any analytical or computational tool that is used to simulate the aerothermal environment must include the proper chemical reactions. The chemical composition of the flowfield strongly affects the flowfield induced emission and absorption of radiation.

The present paper describes a computational method for the simulation of the aerothermal environment around a hypersonic vehicle at high altitude. Traditionally, two types of computational methods are available for such simulations, viz., continuum methods and molecular methods. In a continuum method, the flowfield and its chemical composition are determined via the numerical solution of a system of partial differential equations (PDEs). This approach can be made computationally efficient, using a multitude of techniques, but loses its validity when the flow conditions are such that the hypotheses that underlie the PDEs break down, i.e., at high altitudes (low densities). In a molecular method, such as the direct simulation Monte Carlo (DSMC) method, on the other hand, an attempt is made to model the molecular processes (such as collisions and reactions) directly. This approach is in general less efficient than the continuum approach because the modeling of the molecular collision processes requires time steps to be taken that are of the same order as the intermolecular collision times. At high altitudes, however, these times become large enough so that the method becomes practical. In addition, no restrictions apply to the altitudes at which this approach can be used. Therefore, this method has been applied successfully to the computation of the flowfield around re-entry vehicles.

The approach described in the present paper combines certain aspects of the continuum approach with certain aspects of the molecular approach, in an attempt to retain some of the

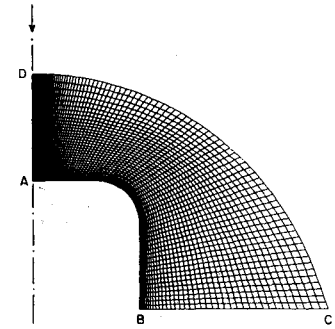

Fig. 1 Computational domain and grid.

Received May 24, 1990; presented as Paper 90-1691 at the AIAA/ASME 5th Joint Thermophysics and Heat Transfer Conference, Seattle, WA, June 18-20, 1990; revision received July 22, 1991; accepted for publication July 24, 1991.

*Senior Research Scientist. Member AIAA.
†Senior Research Scientist; currently at United Technologies Research Center, East Hartford, CT. Member AIAA.
‡Chief Scientific Officer; currently at Applied Research Laboratory, Pennsylvania State University, University Park, PA. Member AIAA.

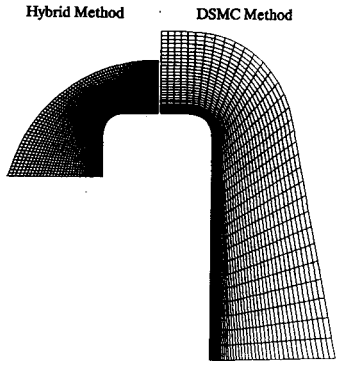

Fig. 2 Grids used in hybrid and DSMC calculations.

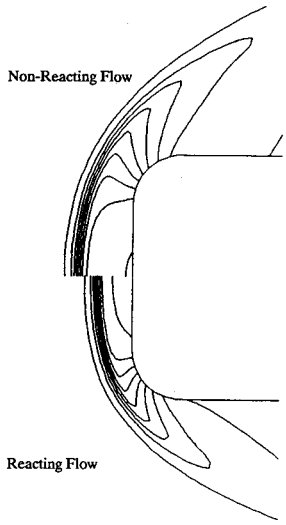

Fig. 3 Pressure contours for reacting and nonreacting flow calculations.

advantages of each of these methods, without being restricted by some of their disadvantages. This "hybrid" approach should therefore be beneficial at intermediate altitudes. In this method, the Navier-Stokes equations are solved numerically for the mean flowfield, together with the global continuity and energy equations for the gas mixture, assuming "frozen" species concentrations. Next, the species transport equations are solved for the species concentrations to account for species convection and diffusion. Finally, a representative set of reactions is computed among computational particles (representing the species molecules) by means of DSMC-like techniques. The postreaction particle distribution is used to update the species concentrations.

The use of a continuum description of the gas mixture and the species transport allows the use of the efficient solution techniques available for the solution of systems of PDEs, while the use of a statistical description of the chemical reactions allows one to include the use of collision/reaction cross sections and/or probabilities (rather than the use of continuum reaction rates). This latter information is (or can be made) available via the use of computational chemistry and facilitates the inclusion of more accurate chemical reaction models, surface catalytic reactions, etc. The hybrid method is not restricted to the same (small) time steps as a molecular (DSMC) method because the collision processes are not modeled and the molecular reaction processes take place on a slower scale than the collision processes in the range of altitudes considered here. The restrictions on the continuum approach, however, remain, insofar as they are related to the intermolecular collision processes (and not the reaction processes).

Under the present study the hybrid method described earlier was applied to the computation of the axisymmetric hypersonic flow about a blunt-faced cylindrical forebody. Since the emphasis in these calculations was on the chemical reaction modeling, a multitemperature model (with additional energy equations for the rotational, vibrational, and electron energies) or a radiation transport model were not included, although the incorporation of these models is needed to obtain a more accurate description of the physical processes. Results of the hybrid method calculations were compared with results of calculations performed using both a full Navier-Stokes method and a DSMC method.

II. Analysis and Governing Equations

The hybrid method developed by de Jong et al.[1] allows the analysis of chemically reacting gas flows around a vehicle traveling at hypersonic speeds within the atmosphere. In this method, the Navier-Stokes equations are used to model the gas flow, whereas a Monte Carlo-like technique is used to simulate the chemical reactions. In the form of the hybrid method used here, three steps are taken for each small time interval Δt:

1) Navier-Stokes phase: Continuity, momentum conservation, and energy conservation equations are solved for the gas mixture of frozen composition. These equations are supplemented by an equation of state, a caloric equation of state, and relations for the mixture viscosity and thermal conductivity.

2) Species transport phase: Conservation equations are solved for the mass fractions of the species that constitute the gas mixture. Relations for the diffusivities complement these equations.

3) Chemical reaction phase: Species production due to chemical reactions is computed via a statistical (Monte Carlo) method. Information about either continuum reaction rates or molecular reaction cross sections (or probabilities) is used to define the reaction statistics.

A detailed description of each of the steps of the hybrid Navier-Stokes/Monte Carlo method is presented next.

Navier-Stokes Phase

In the Navier-Stokes phase, the mean flowfield calculations are performed via numerical solution of the Navier-Stokes equations and the global continuity and energy equations for the gas mixture. In vector form this set of equations can be written as

$$\frac{\partial \rho}{\partial t} + \nabla \cdot \rho U = 0 \tag{1}$$

$$\frac{\partial (\rho U)}{\partial t} + \nabla \cdot (\rho UU) = -\nabla p + \nabla \cdot \tau \tag{2}$$

$$\frac{\partial (\rho h_0)}{\partial t} + \nabla \cdot (\rho U h_0) = \frac{\partial p}{\partial t} - \nabla \cdot (\tau \cdot U) - \nabla \cdot q + \dot{q}_r \tag{3}$$

where q_r is the radiation term.

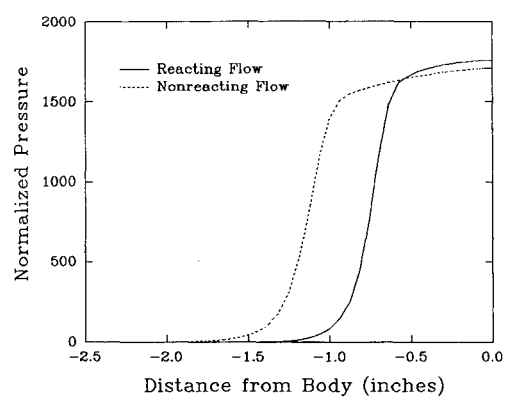

Fig. 4 Pressure profile along the stagnation streamline.

The multicomponent energy flux consists of a conductive energy flux (heat flux), an interdiffusional energy flux, and a Dufour energy flux. The latter is quite complex in nature and usually of minor importance (cf. Bird et al.[2]) and has therefore been neglected. Then q reduces to

$$q = -k\nabla T + \sum_{i=1}^{N} h_i j_i \tag{4}$$

where j_i is the diffusional mass flux of species i, which will be discussed in the next section.

The previous equations for the gas mixture have to be supplemented by the equation of state for a perfect gas mixture,

$$\frac{p}{\rho} = RT\sum_{i=1}^{N}\frac{Y_i}{M_i} = \frac{RT}{\sum_{i=1}^{N} X_i M_i} \tag{5}$$

The temperature T is related to the mixture enthalpy h via the caloric equation of state

$$h = \sum_{i=1}^{N} Y_i\left[h_{f_i} + \int_{T_{f_i}}^{T} c_{p_i}(s)\,ds\right] \tag{6}$$

Values of h_{f_i} and T_{f_i} and empirical relations between c_p and T for different species can be found in Benson[3] and the JANNAF tables.[4]

To complete the set of Eqs. (1-6), formulas are needed for the mixture viscosity μ (which appears in the stress tensor τ) and the mixture thermal conductivity k (which appears in the energy flux vector q). By the semi-empirical formula of Wilke,[5]

$$\mu = \sum_{i=1}^{N}\frac{X_i\mu_i}{\sum_{j=1}^{N} X_j\Phi_{ij}} \tag{7}$$

where Φ_{ij} is given by

$$\Phi_{ij} = \frac{1}{8^{1/2}}\left(1+\frac{M_i}{M_j}\right)^{-1/2}\times\left[1+\left(\frac{\mu_i}{\mu_j}\right)^{1/2}\left(\frac{M_j}{M_i}\right)^{1/4}\right]^2 \tag{8}$$

The viscosity of a single species can be determined from the kinetic theory expression (e.g., Bird et al.[2] or Hirschfelder et al.[6]):

$$\mu_i = 266.93\ 10^{-7}\frac{(M_i T)^{1/2}}{\sigma_i^2\,\Omega_{v_i}} \tag{9}$$

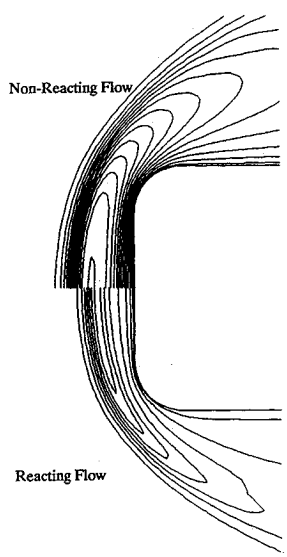

Fig. 5 Temperature contours for reacting and nonreacting flow calculations.

Table 1 Flow conditions

Altitude, km	80
Pressure, N/m^2	1
Temperature, K	181
Density, kg/m^3	2.10^{-5}
Number density, m^{-3}	$4.2\ 10^{20}$
Mean free path, m	$4.1\ 10^{-3}$
Mass fractions	
O_2	0.233
N_2	0.767
Velocity, km/s	10
Mach number	37

where μ_i is given in g/cm-s, T is given in K, σ_i is a molecular collision diameter (in Angstrom), and Ω_{v_i} is a viscosity collision integral, which can be approximated by (cf. White[7])

$$\Omega_{v_i} \approx 1.147\left(\frac{T}{T_{\epsilon_i}}\right)^{-0.145} + \left(\frac{T}{T_{\epsilon_i}}+0.5\right)^{-2} \tag{10}$$

Here T_{ϵ_i} is a molecular temperature diameter. Values for σ_i and T_{ϵ_i} can be found in Svehla.[8]

Finally, the thermal conductivity k is given by Eucken's approximation (cf. Bird et al.[2]),

$$k = \sum_{i=1}^{N}\frac{X_i k_i}{\sum_{j=1}^{N} X_j\Phi_{ij}} \tag{11}$$

where k_i is the thermal conductivity of species i given by

$$k_i \approx \left(C_{p_i} + \frac{5}{4}\frac{R}{M_i}\right)\mu_i \tag{12}$$

and where Φ_{ij} is the same function as in Eqs. (7) and (8).

The radiation source term in the energy equation (3) has to be obtained from a radiation transport model. Because the emphasis in the present study was on the chemical reaction modeling, this radiation term was not included. Moreover, the flow was assumed to be laminar in the high-altitude forebody calculations considered here.

In summary, the system of equations used in the present effort consists of the partial differential equations (1-3) and the auxiliary relations (4-12). Given the mole fractions of each of the species of the mixture (or, equivalently, given the mass fractions), these equations can be solved for the mixture properties ρ, U, h, p, and T.

The numerical method used to solve the system of equations is based on the finite difference approach discussed by Briley and McDonald,[9,10] which uses a consistently split, linearized block-implicit (LBI) ADI procedure. The LBI scheme, being an implicit method, does not suffer from the stability restrictions that relate the temporal step to the spatial mesh size. This is an important advantage in view of the existence of high characteristic velocities and the need to use locally refined meshes for accurate prediction of the flowfield near solid surfaces and in the regions of sharp temperature or species concentration gradients. Further, the solution procedure treats the nonlinearities *noniteratively* by Taylor series linearization to the requisite order in time and then by splitting the matrix into a series of easily solved block-banded subsystems. The solution procedure is, thus, computationally efficient. Further details on the LBI algorithm are available in Briley and McDonald.[9,10]

Species Transport Phase

The species transport phase can be treated either by a discrete method or by a continuum method. In the discrete method, computational particles representing the species molecules are transported using convection velocities com-

Table 2 List of chemical reactions, five-species model[a]

No.	Reaction	Rate coefficient, in m³/molecule-s $aT^b \exp(-c/T)$		
		a	b	c
1	$O_2+N \rightarrow 2O+N$	5.993×10^{-12}	−1.0	59,370
2	$O_2+NO \rightarrow 2O+NO$	5.993×10^{-12}	−1.0	59,370
3	$O_2+N_2 \rightarrow 2O+N_2$	1.198×10^{-11}	−1.0	59,370
4	$O_2+O_2 \rightarrow 2O+O_2$	5.393×10^{-11}	−1.0	59,370
5	$O_2+O \rightarrow 2O+O$	1.498×10^{-10}	−1.0	59,370
6	$N_2+O \rightarrow 2N+O$	3.187×10^{-13}	−0.5	113,000
7	$N_2+O_2 \rightarrow 2N+O_2$	3.187×10^{-13}	−0.5	113,000
8	$N_2+NO \rightarrow 2N+NO$	3.187×10^{-13}	−0.5	113,000
9	$N_2+N_2 \rightarrow 2N+N_2$	7.968×10^{-13}	−0.5	113,000
10	$N_2+N \rightarrow 2N+N$	6.900×10^{-8}	−1.5	113,000
11	$NO+N_2 \rightarrow N+O+N_2$	6.590×10^{-10}	−1.5	75,550
12	$NO+O_2 \rightarrow N+O+O_2$	6.590×10^{-10}	−1.5	75,550
13	$NO+NO \rightarrow N+O+NO$	1.318×10^{-8}	−1.5	75,550
14	$NO+O \rightarrow N+O+O$	1.318×10^{-8}	−1.5	75,550
15	$NO+N \rightarrow N+O+N$	1.318×10^{-8}	−1.5	75,550
16	$NO+O \rightarrow O_2+N$	5.279×10^{-21}	1.0	19,700
17	$N_2+O \rightarrow NO+N$	1.120×10^{-16}	0.0	37,500
18	$O_2+N \rightarrow NO+O$	1.598×10^{-18}	0.5	3,600
19	$NO+N \rightarrow N_2+O$	2.490×10^{-17}	0.0	0

[a]Without three-body recombination reactions that do not participate at low densities.

puted in the Navier-Stokes phase, taking into account molecular diffusion of the species. This approach, which is described in detail by de Jong et al.,[1] is advantageous when the number of species is large. In the continuum method, on the other hand, species transport is accounted for by the numerical solution of a set of convection/diffusion equations for the species concentrations. This approach is more economical when the number of species is not too large and allows the use of the same numerical techniques as those applied to the solution of the Navier-Stokes equations. Therefore, the continuum method was chosen for the present effort.

The set of species transport equations can be written in the form

$$\frac{\partial(\rho Y_i)}{\partial t} + \nabla\cdot(\rho U Y_i) = -\nabla\cdot\left(j_i - \frac{1}{N}\sum_{k=1}^{N} j_k\right) + r_i \qquad (13)$$

The right-hand side of Eq. (13) has been written to guarantee consistency of the species transport equations with the continuity equation for the mixture.

The diffusion mass flux consists of four terms: ordinary (concentration) diffusion, pressure diffusion, forced diffusion, and thermal diffusion (the Soret effect). In the absence of pressure, forced, or temperature diffusion, the diffusion mass flux j_i simplifies to

$$j_i = -\rho D_i \nabla Y_i \qquad (14)$$

In this relation, the diffusivity D_i of the species i into the mixture can be determined from the following relation (cf. Bird et al.[2]):

$$D_i \approx \frac{1-X_i}{\sum_{\substack{j=1\\ j\neq 1}}^{N}\left(\frac{X_j}{D_{ij}}\right)} \qquad (15)$$

where D_{ij} is the binary diffusion coefficient of species i into species j, which can be expressed as

$$D_{ij} = \frac{0.001858\, T^{3/2}\left(1/M_i + 1/M_j\right)^{1/2}}{p\sigma_{ij}^2\Omega_D} \qquad (16)$$

Here D_{ij} is in cm²/s, p in atm, T in K, and σ_{ij}—the effective collision diameter, given by $\sigma_{ij} = \frac{1}{2}(\sigma_i + \sigma_j)$, where σ_i is the molecular collision diameter of species i—in Å. The diffusion collision integral Ω_D can be approximated by (cf. White[7])

$$\Omega_D \approx \left(\frac{T}{T_{\epsilon_{ij}}}\right)^{-0.145} + \left(\frac{T}{T_{\epsilon_{ij}}} + 0.5\right)^{-2.0} \qquad (17)$$

where

$$T_{\epsilon_{ij}} = \left(T_{\epsilon_i} T_{\epsilon_j}\right)^{1/2} \qquad (18)$$

where T_{ϵ_i} is the molecular temperature diameter of species i. The values of σ and T_ϵ used in the computation of the diffusivities via Eqs. (16-18) are the same as those used in the computation of the viscosities via Eqs. (9) and (10).

In a full continuum (Navier-Stokes) method, the rate of production r_i in Eq. (13) is obtained using the relevant set of chemical reactions and the corresponding reaction rate coefficients (cf. Vincenti and Krueger[11]). In the present form of the hybrid method, however, the species transport phase and the chemical reaction phase are decoupled (much as in a DSMC method), and the effect of chemical reactions on the species concentrations is computed separately, i.e., $r_i = 0$ in Eq. (13).

Chemical Reaction Phase

In the reaction phase, a representative set of reactions that takes place in the time interval Δt is computed among computational particles by means of techniques similar to those used in DSMC methods. In these methods, nonequilibrium chemical reactions are readily handled by procedures that are essentially extensions of the elementary collision theory of chemical physics. The binary reaction rate is obtained as the product of the collision rate for collisions with energy in excess of the activation energy and the probability of reaction. Since the

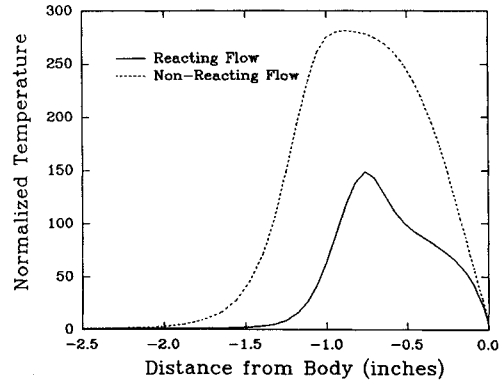

Fig. 6 Temperature profile along the stagnation streamline.

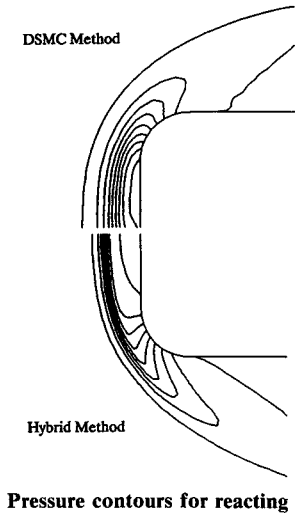

Fig. 7 Pressure contours for reacting flow calculations.

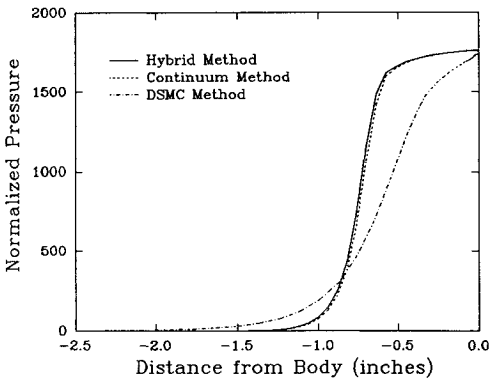

Fig. 8 Pressure profile along the stagnation streamline (reacting flow).

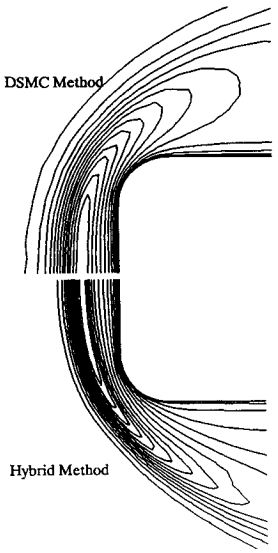

Fig. 9 Temperature contours for reacting flow calculations.

formulation is in terms of kinetic theory, the model can be incorporated directly into a DSMC method.

Although the reaction cross sections (or probabilities) may be available directly from the thermophysical database, the chemical data for gas phase reactions is almost invariably quoted in terms of reaction rate constants (see, for example, Lee,[12] Park,[13] Shinn et al.,[14] and Sturtevant and Steinhilper[15]). These temperature dependent rate constants of continuum theory can be converted into collision energy dependent reaction cross sections (cf. Bird[16]). This procedure is followed by the present approach. Only binary reactions are considered because recombination reactions are not important at very low densities where the probability of three-body collisions is extremely small. They become important in the continuum overlap region and could be dealt with by assigning a lifetime to each binary collision and regarding the ternary collision as a binary collision between the pair of molecules in the original collision and a third molecule. Such a procedure can be incorporated in a form that guarantees the correct equilibrium state (cf. Bird[17]).

The numerical scheme consists of the following steps (for each mesh cell):

1) Pick a reaction among the set of all binary reactions under consideration, say $A+B \rightarrow C+D$.

2) Pick one particle of each of the (two) species A and B. Note that the statistical weight of these particles (i.e., the number of physical molecules that they represent) must be the same. In the DSMC method, the particles chosen have velocities associated with them. In the present method, the choice of a particle includes the choice of velocity components from the appropriate (for example, Maxwellian) molecular velocity distribution.

3) Determine the reaction cross section.

4) Based on the reaction probability, which relates directly to the reaction cross section, determine whether or not a reaction takes place.

5) If a reaction takes place, create particles of the species C and D, and omit the particles of species A and B. In other words, update the species concentrations. In addition, update a reaction time counter for the particular reaction by an amount inversely proportional to the reaction probability.

6) Omit the reaction from the set of reactions under consideration if its time counter exceeds the physical time.

7) Repeat the procedure until the set of reactions is empty, i.e., until the reaction time counters for all reactions have exceeded the physical time.

The use of reaction time counters ensures that, over a large number of reactions, the procedure leads to a reaction rate that is in agreement with the reaction cross section (cf. Bird[16]). This leads to an interesting observation: if the reaction cross sections are determined such that the resulting reaction rates correspond to those of continuum theory, then the steps (2-5) in the previous procedure could be replaced by the following step.

5)* Let a reaction take place. Update the species concentrations; update the reaction time counter by an amount inversely proportional to the reaction rate.

In that case, the procedure can be considered as a stochastic method for solving a system of ordinary differential equations of the form

$$\frac{dn_A}{dt} = -\sum_B n_A n_B k_{AB}(T) + \sum_{C,D} n_C n_D k_{CD}(T) \qquad (19)$$

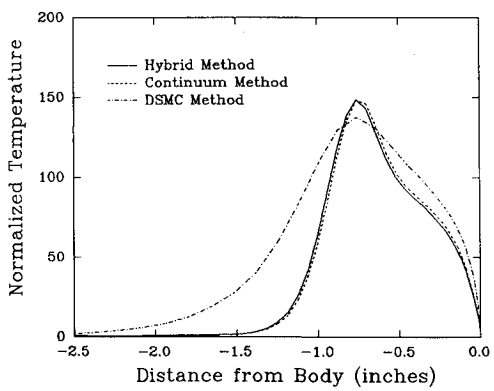

Fig. 10 Temperature profile along the stagnation streamline (reacting flow).

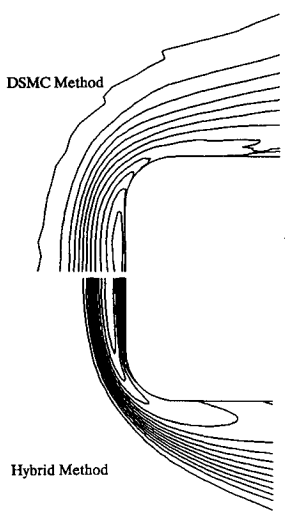

Fig. 11 N_2 mass fraction contours.

The first sum on the right-hand side of Eq. (19) is over all reactions of the form $A + B \rightarrow \ldots$, while the second sum is over all reactions of the form $C + D \rightarrow A + \ldots$.

The advantage of using the complete procedure (1-7) rather than the simplified one (with 2-5 replaced by 5*) lies in the fact that alternative formulations for the reaction cross sections, based on molecular models rather than continuum theory, can be implemented easily.

III. Application and Results

The hybrid method described previously was applied to the computation of the axisymmetric hypersonic flow about a blunt-faced cylindrical forebody. The forebody consists of a 5-in. diameter circular cylinder with a 3-in. diameter circular front face and a 1-in. radius of curvature transition from the front face to the cylindrical part of the body. Table 1 lists the relevant flow conditions, while Fig. 1 shows the geometry and the computational grid used. In this figure, AD is on the axis of symmetry, BC is the "downstream" boundary of the computational grid, and DC is the "upstream"/"far-field" boundary, chosen such that it is an inflow boundary. The bow shock wave intersects the downstream boundary. The grid used consists of 100 mesh points along the body and 50 mesh points in the normal direction concentrated near the body surface (AB in Fig. 1) and the stagnation point (A in Fig. 1), to allow proper resolution of the boundary layer and the stagnation point region.

The body surface was assumed to be noncatalytic and was kept at a temperature of 300 K. No-slip conditions (both on temperature and velocity) were applied on this surface, and the normal derivatives of the species mass fractions were set to zero. The chemical reaction set considered consists of 19 reactions for 5 species (N_2, O_2, NO, N, and O) and was adopted from Moss et al.,[18] where it has been used in calculations of the flowfield around the Aeroassist Flight Experiment (AFE) vehicle at altitude and speed ranges of 78-90 km and 7.6-9.9 km/s, respectively. Table 2 lists the relevant data. Three-body atom recombination reactions are not significant at high altitudes and have not been included.

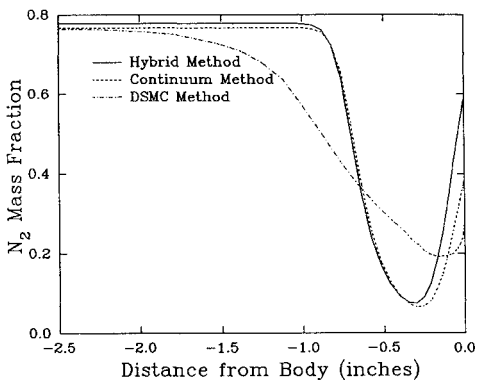

Fig. 12 N_2 mass fraction profile along the stagnation streamline.

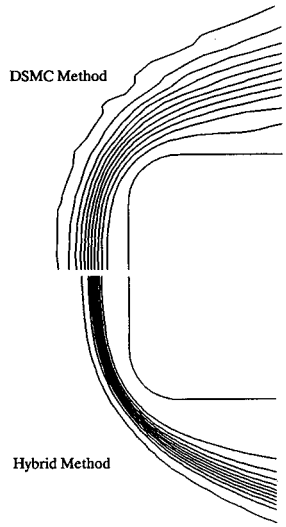

Fig. 13 O_2 mass fraction contours.

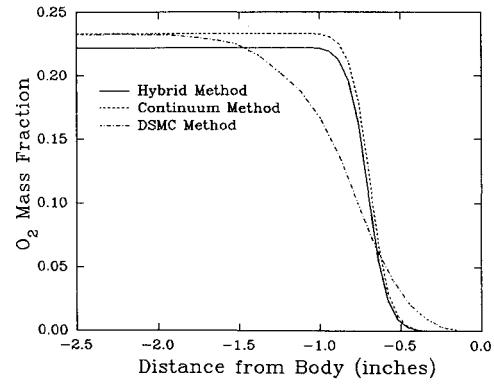

Fig. 14 O_2 mass fraction profile along the stagnation streamline.

To assess the validity of the results obtained with the hybrid method, the reacting flow calculations were compared with results obtained by using both a full Navier-Stokes method and a DSMC method with the same chemical reaction set. The continuum method corresponds to the first two phases of the hybrid method, with the appropriate species production rate terms included in Eq. (13) (cf. Sec. II). The DSMC calculations (cf. Bird[16]) were performed on a grid using 40×33 mesh cells, shown in Fig. 2 in comparison with the grid used in the hybrid code calculations (identical to the one shown in Fig. 1). Although the two grids are quite dissimilar, their resolution is comparable.

Results of the computations are shown in Figs. 3-14. In Figs. 3-6, pressure and temperature (both normalized by their freestream values) are compared for calculations done with and without chemical reactions using the hybrid code. It should be noted here that the hybrid method reduces to a continuum method if there are no chemical reactions. Figures 3 and 4 show that the pressure behind the bow shock is similar for the reacting and nonreacting flow but that the shock standoff distance is smaller when the chemical reactions are included. The need to include real gas effects is quite evident in Figs. 5 and 6, which show the temperature distributions. The peak temperature predicted by the reacting flow simulation is significantly lower than that predicted by the nonreacting flow simulation, due to the effect of the endothermic reactions.

Figures 7-10 compare the pressure and temperature obtained by using the hybrid code, the Navier-Stokes code, and the DSMC code. As can be seen in Figs. 8 and 10, results from the hybrid code and the Navier-Stokes code are almost identical. Figures 7 and 8 indicate that the pressure rise through the bow shock predicted by the hybrid and DSMC methods is quite similar. The DSMC calculations, however, lead to a thicker shock. It should be emphasized here that the shock thickness in the hybrid solution is largely due to the effect of the numerical dissipation in the Navier-Stokes part of the calculation procedure, which was kept to a minimum (while still retaining numerical stability). The shock thickness obtained from a continuum approach can always be increased by increasing the numerical dissipation. The results obtained in such a way, however, have no relationship to the physics of the flow. The larger shock thickness predicted by the DSMC calculations, on the other hand, is a direct result of the large mean free path at 80 km altitude (cf. Bird[19]). In view of the large mean free path, the thicker shock predicted by the DSMC method is believed to be physically more realistic.

A comparison of the temperature field predicted by the hybrid and the DSMC codes is presented in Figs. 9 and 10.

The magnitude and the location of the temperature peak predicted by the two methods agree quite favorably. However, the thicker shock predicted by the DSMC method results in the temperature rise predicted by this method being spread over a larger distance. Further, a closer examination of Fig. 10 reveals that the DSMC calculations predict a temperature jump of about 1000 K at the body surface. This phenomenon is a direct consequence of the local Knudsen number not being negligibly small, since the ratio of the temperature jump to the gas temperature should be of the same order as the local Knudsen number. The occurrence of this temperature jump is an indication of the fact that the continuum approach is starting to break down at this altitude. Suitable models for the surface temperature (and velocity) jump need to be incorporated into the hybrid method to increase its accuracy at high altitudes (cf. Gupta et al.,[20] Shinn and Simmonds[21]).

The distributions of N_2 and O_2 mass fractions and the corresponding profile plots along the stagnation streamline are shown in Figs. 11-14. Again, the results obtained with the hybrid and Navier-Stokes codes are almost identical, whereas the results obtained with the DSMC code show some differences as a result of the larger shock thickness and the surface temperature jump. The larger shock thickness in the DSMC result leads to smaller gradients of the mass fractions across the bow shock, whereas the surface temperature jump results in higher surface N_2 dissociation, leading to lower N_2 concentrations at the surface. Both calculations predict complete dissociation of O_2 at the front face. The slightly different freestream species concentrations in the hybrid calculations (cf. Figs. 12 and 14), which correspond to a 20% volume fraction of O_2 rather than a 21% volume fraction, do not seem to significantly affect these results. Predicted distributions of mass fractions of N, O, and NO from these three methods show similar behavior and have been discussed by de Jong et al.[22]

IV. Conclusions

The chemically reacting flow about a blunt-faced cylindrical forebody traveling at hypersonic speed and high altitude has been simulated using a newly developed hybrid Navier-Stokes/Monte Carlo method. The results of the computations are almost identical to those obtained with a full continuum (Navier-Stokes) method. Comparison with results obtained using a direct simulation Monte Carlo method shows good agreement, except where the assumptions underlying the continuum approach are starting to break down: the DSMC results show a larger shock thickness and a surface temperature jump that result in some differences in the predictions for the species mass fraction distributions. The hybrid method uses a statistical description of the chemical reactions that allows one to include the use of collision/reaction cross sections and/or reaction probabilities (available via the use of computational chemistry) and facilitates the inclusion of more accurate chemical reaction models, surface catalytic reactions, etc.

Acknowledgments

This research was supported by the Air Force Armament Laboratory under Contract No. F08635-87-C-0003 via a subcontract through Science Applications International Corporation and by the Army Research Office under Contract No. DAAL03-88-C-0028. The authors would also like to thank Graeme A. Bird for his helpful discussions regarding the DSMC calculations.

References

[1]De Jong, F. J., Sabnis, J. S., and McDonald, H., "Hypersonic Vehicle Environment Simulation," Scientific Research Associates, Final Rept. No. R89-930019-F, ARO Contract DAAL03-88-C-0028, Glastonbury, CT, May 1989.

[2]Bird, R. B., Stewart, W. E., and Lightfoot, E. N., *Transport Phenomena,* Wiley, New York, 1960, pp. 563-568.

[3]Benson, R. S., *Advanced Engineering Thermodynamics,* Pergamon Press, Oxford, England, UK, 1977, pp. 270-271.

[4]Chase, M. W., *JANNAF Thermochemical Tables,* Dow Chemical Co., Midland, MI, 1965.

[5]Wilke, C. R., "A Viscosity Equation for Gas Mixtures," *Journal of Computational Physics,* Vol. 18, No. 4, 1950, pp. 517-519.

[6]Hirschfelder, J. O., Curtiss, C. F., and Bird, R. B., *The Molecular Theory of Gases and Liquids,* Wiley, New York, 1954, pp. 514-610.

[7]White, F. M., *Viscous Fluid Flow,* McGraw-Hill, New York, 1974, pp. 27-36.

[8]Svehla, R. A., "Estimated Viscosities and Thermal Conductivities of Gases at High Temperatures," NASA TR R-132, 1962.

[9]Briley, W. R., and McDonald, H., "Solution of the Multidimensional Compressible Navier-Stokes Equations by a Generalized Implicit Method," *Journal of Computational Physics,* Vol. 24, No. 4, 1977, pp. 372-397.

[10]Briley, W. R., and McDonald, H., "On the Structure and Use of Linearized Block Implicit Schemes," *Journal of Computational Physics,* Vol. 34, No. 1, 1980, pp. 54-73.

[11]Vincenti, W. G., and Krueger, C. H., *Introduction to Physical Gas Dynamics,* Wiley, New York, 1965, pp. 197-244.

[12]Lee, J. H., "Basic Governing Equations for the Flight Regimes of Aeroassisted Orbital Transfer Vehicles," *Thermal Design of Aeroassisted Orbital Transfer Vehicles,* edited by H. F. Nelson, Vol. 96, Progress in Astronautics and Aeronautics, AIAA, New York, 1984, pp. 3-53.

[13]Park, C., "Problems of Rate Chemistry in the Flight Regimes of Aeroassisted Orbital Transfer Vehicles," *Thermal Design of Aeroassisted Orbital Transfer Vehicles,* edited by H. F. Nelson, Vol. 96, Progress in Astronautics and Aeronautics, AIAA, New York, 1984, pp. 511-537.

[14]Shinn, J. L., Moss, J. N., and Simmonds, A. L., "Viscous Shock-Layer Heating Analysis for the Shuttle Windward Plane with Surface Finite Catalytic Recombination Rates," AIAA Paper 84-0842, June 1982.

[15]Sturtevant, B., and Steinhilper, E. A., "Intermolecular Potentials from Shock Structure Experiments," *Rarified Gas Dynamics,* edited by K. Karamcheti, Academic Press, New York, 1974, pp. 159-166.

[16]Bird, G. A., *Molecular Gas Dynamics,* Clarendon Press, Oxford, England, UK, 1976, pp. 190-200.

[17]Bird, G. A., "Direct Molecular Simulation of a Disassociating Diatomic Gas," *Journal of Computational Physics,* Vol. 25, No. 3, 1977, p. 405.

[18]Moss, J. N., Bird, G. A., and Dogra, V. K., "Non-Equilibrium Thermal Radiation for an Aeroassist Flight Experiment Vehicle," AIAA 26th Aerospace Sciences Meeting, AIAA Paper 88-0081, Reno, NV, Jan. 1988.

[19]Bird, G. A., "Aspects of the Structure of Strong Shock Waves," *Physics of Fluids,* Vol. 13, No. 5, May 1970, pp. 1172-1177.

[20]Gupta, R. N., Scott, C. D., and Moss, J. N., "Surface-Slip Equations for Low Reynolds Number Multicomponent Air Flow," *Thermal Design of Aeroassisted Orbital Transfer Vehicles,* edited by H. F. Nelson, Vol. 96, Progress in Astronautics and Aeronautics, AIAA, New York, 1984, pp. 465-490.

[21]Shinn, J. L., and Simmonds, A. L., "Comparison of Viscous Shock Layer Heating Analysis with Shuttle Flight Data in Slip Flow Regime," *Thermal Design of Aeroassisted Orbital Transfer Vehicles,* edited by H. F. Nelson, Vol. 96, Progress in Astronautics and Aeronautics, AIAA, New York, 1984, pp. 491-510.

[22]De Jong, F. J., Sabnis, J. S., Buggeln, R. C., and McDonald, H., "Hypersonic Flow Calculations with a Hybrid Navier-Stokes/Monte Carlo Method," AIAA Paper 90-1691, June 1990.

Ernest V. Zoby
Associate Editor